University of Baghdad
College of Engineering
JE
JOURNAL OF ENGINEERING

Journal of Engineering
journal homepage: www.joe.uobaghdad.edu.iq
Number 7 Volume 26 July 2020

Electrical, Electronics and communications, and Computer Engineering

Bat Algorithm Based an Adaptive PID Controller Design for Buck Converter Model

Luay Thamir Rasheed
Assistant Lecturer
Control & Systems Eng. Dept.-University of Technology
Iraq, Baghdad
60065@uotechnology.edu.iq

ABSTRACT

The aim of this paper is to design a PID controller based on an on-line tuning bat optimization algorithm for the step-down DC/DC buck converter system which is used in the battery operation of the mobile applications. In this paper, the bat optimization algorithm has been utilized to obtain the optimal parameters of the PID controller as a simple and fast on-line tuning technique to get the best control action for the system. The simulation results using (Matlab Package) show the robustness and the effectiveness of the proposed control system in terms of obtaining a suitable voltage control action as a smooth and unsaturated state of the buck converter input voltage of (3.75) volt that will stabilize the buck converter system performance. The simulation results show also that the proposed control system when compared with the other controllers results has the capability of minimizing the rising time to (0.393×10^{-4} sec) and the settling time to (2×10^{-4} sec) in the transient response and minimizing the voltage tracking error of the system output to ($zero$) volt at the steady state response. Furthermore, the number of fitness evaluations is decreased.

Keywords: Bat Algorithm, Buck Converter, State Space Averaging, On-Line-Tuning Optimization.

تصميم المسيطر التناسبي التكاملي التفاضلي المتكيف المبني على اساس خوارزمية الخفافيش للمبدل الخافض للجهد المستمر

لؤي ثامر رشيد
مدرس مساعد
قسم هندسة السيطرة والنظم
الجامعة التكنولوجية

الخلاصة

تهدف هذه الورقة الى تصميم المسيطر التناسبي التكاملي التفاضلي المتكيف وبشكل حي متصل لمبدل خفض الجهد المستمر الذي يستخدم في عمل البطارية في التطبيقات النقالة. في هذه الورقة البحثية تم استخدام خوارزمية الخفافيش لايجاد و تنغيم المعلمات المثلى للمسيطر كطريقة تنغيم بسيطة وسريعة وبشكل حي متصل للحصول على اقضل فولتية فعل سيطرة لتحقيق الاداء المطلوب لخراج مبدل الخفض. ان نتائج المحاكاة باستخدام برنامج الماتلاب للمسيطر التناسبي التكاملي التفاضلي المتكيف مع خوارزمية

*Corresponding author
Peer review under the responsibility of University of Baghdad.
https://doi.org/10.31026/j.eng.2020.07.05

Article received: 15/10/2019
Article accepted:22/12/2019
Article published:1/7/2020

الخفافيش المستخدمة بشكل حي متصل اظهرت متانة وفعالية المسيطر المقترح من حيث الحصول على على افضل فولتية فعل سيطرة ناعمة وبدون حالة الاشباع من فولتية المصدر لمبدل خفض الجهد المستمر والبالغة 3.75 فولت التي تجعل اداء المسيطر مستقرا. اظهرت نتائج المحاكاة ايضا ان نتائج المسيطر المقترح عند مقارنتها مع نتائج المسيطرات الاخرى ان المسيطر المقترح له القابلية على تقليل كل من زمن الارتفاع الى (0.393×10^{-4}) ثانية و زمن الاستقرار الى (2×10^{-4}) ثانية في استجابة الحالة المؤقتة وكذلك تقليل تتابع الخطأ لفولتية الخراج لمبدل الخفض الى صفر فولت في استجابة الحالة المستقرة. علاوة على ذلك يتم تقليل رقم دالة التقييم.
الكلمات الرئيسية: خوارزمية الخفافيش، مبدل خفض الجهد المستمر ، متوسط فضاء الحالة، الضبط الامثل بشكل حي متصل.

1. INTRODUCTION

In the last few decades, DC/DC converters have been playing an important role in our life because of its essential use in mobile applications such as computer systems, portable devices, etc. Therefore, the control of these circuits for mobile applications is needed so as to get a voltage regulation with the high conversion efficiency and fast transient response **(Abed, et al., 2018)** and **(Chander, et al., 2013).**

Buck converter is one of these DC/DC converters which steps down a given DC value (source voltage) into the desired regulated DC output value. The buck converter's output voltage at the load is controlled by varying (modulating) the width of the switch chopped input pulse, which is controlling the duration of the time the electronic switches, MOSFETs, are ON or OFF in one cycle of the operating frequency; this is known as pulse width modulation **(Lv, et al., 2015).**

According to the importance of the buck converters in many industrial and residential applications, a vast amount of control algorithms for these converters have been devoted to their control in order to obtain a fast dynamic response and desired output voltage with variable load current. For instance, sliding model controller, **(Chafekar and Mate, 2018)**, adaptive hysteresis controllers, **(Kim, et al., 2012),** fuzzy logic controller, (**Tapou, et al., 2011)**, PWM with dead time controller based FPGA **(Themozhi and Reddy, 2014),** adaptive backstepping control using chebyshev neural network, **(Nizami and Mahanta, 2014),** observer controller, **(Lakshmi and Raja, 2014),** PI-Lead Compensator, **Garg, et al., 2015**, direct pole placement controller **(Mazlan, et al., 2015),** Modified Elman Neural-PID Controller, (**Dagher, K., 2018)** and model predictive controller, **(Danayiyen, et al., 2017).**

The main core of the motivation for this work is to deal with the problems that influence the operation of the portable devices by controlling the buck converter dynamic behavior in the closed loop system such as wide range of loading current and variable output voltage values. Therefore, the on-line bat optimization algorithm with the PID controller is proposed in this work.

The main points of the contributions of this work are listed as follows:

- The bat optimization algorithm is used because it shows fast search ability in the global regions and rapidly on-line tunes the PID controller optimal gains. These optimal gains lead to finding the optimal voltage control law which leads the buck converter output voltage to attain rapidly the reference output voltage.
- The adaptation performance of the PID controller based on-line bat algorithm is investigated by changing the buck converter output voltage levels.

The remainder of this paper is organized in the following manner: Section two, contains the mathematical model of the synchronous buck converter system. Section three, describes the derivation of the adaptive PID controller. The bat optimization algorithm is explained in section four. Section five presents the numerical simulation results and discussion for the proposed adaptive controller. Finally, the conclusions are explained in section six.

2. MODELING OF THE SYNCHRONOUS BUCK CONVERTER CIRCUIT

The DC/DC buck converter can be considered as a type of attenuation or chopper circuits, whose output voltage is less than the input voltage, so it is otherwise known as step down converter. The simplified circuit of the synchronous DC/DC buck convertor model that is operating in continuous conduction mode (CCM) with the two n-channel MOSFETs Q1 and Q2 controllable switches is shown in **Fig. 1**, **(Al-Araji, 2017).**

This type of buck converter replaces the diode rectifier by the Q2 MOS synchronous rectifier which increases the circuit efficiency and the converter uses one inductor and one capacitor as energy storing elements. Though the converter contains L & C, the system becomes non-linear. Therefore the non-linear system is characterized as linear model within certain range and time-period by using the state space averaging (SSA) technique which is a very common solution.

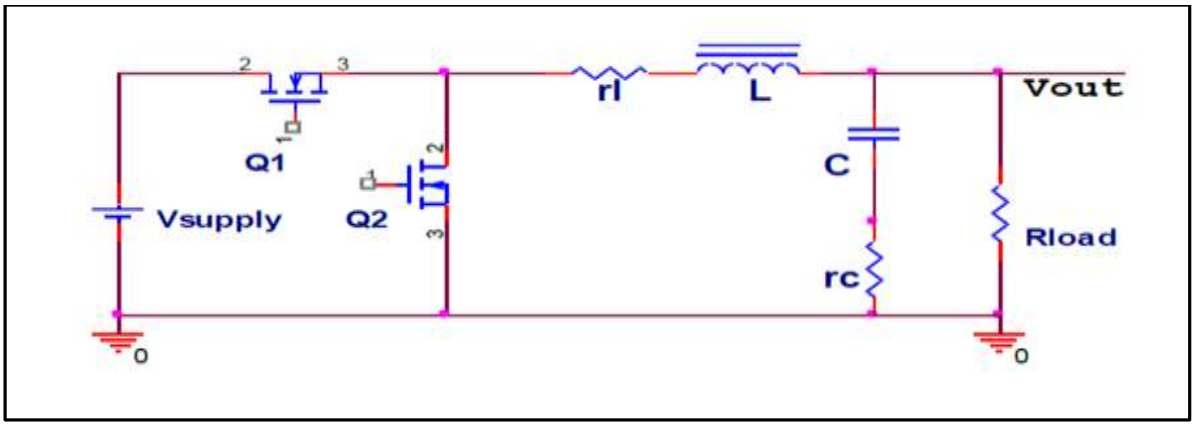

Figure 1. The synchronous buck convertor model.

In CCM, the buck converter operates in two switching modes as follows (**Garg, et al., 2015)** and **(Al-Araji, 2017)**:

(a)When switch Q1 is ON and switch Q2 is OFF for time 0 < t < DT:

At this period of time, the inductor current, capacitor voltage and output voltage equations are given as follows:

$$L\frac{di_L}{dt} = -\left(r_{son} + r_L + \frac{r_c.R_L}{R_L+r_c}\right).i_L - \frac{R_L}{R_L+r_c}v_c + V_s \quad (1)$$

$$C\frac{dV_c}{dt} = \frac{R_L}{R_L+r_c}i_L - \frac{1}{R_L+r_c}v_c \quad (2)$$

$$V_{out} = \frac{r_c.R_L}{R_L+r_c}i_L + \frac{R_L}{R_L+r_c}v_c \quad (3)$$

Where V_s: is the input voltage; i_L: is the inductor current; r_{son}: is the on n-channel resistance of the MOSFET; r_L: is inductor effective series resistance; V_{out}: is the output voltage of the circuit; R_L: is the load resistor; v_c: is the capacitor voltage; r_c: is capacitor effective series resistance; i_c: is capacitor current; C: is the main capacitor; and L: is the main inductance.

(b)When switch Q1 is OFF and switch Q2 is ON for time DT < t < T:

At this period of time, the inductor current is given by Eq. (4) as follows:

$$L\frac{di_L}{dt} = -\left(r_{son} + r_L + \frac{r_c.R_L}{R_L+r_c}\right).i_L - \frac{R_L}{R_L+r_c}v_c \quad (4)$$

The capacitor voltage and output voltage equations are given by equations (2) and (3), respectively.

In this work, to design adaptive PID controller for DC/DC buck convertor, the transfer function of the duty-cycle to output voltage is required. The SSA technique is used for this purpose. Therefore, the buck converter model represented by Eqs. (1, 2, 3, and 4) are symbolized in matrix form as follows **(Garg, et al., 2015**, **Mohan, et al., 1995** and **Kalita, et al., 2015)**:
For switching mode (a),

$$\dot{x}(t) = A_1 x(t) + B_1 u(t) \tag{5}$$

$$y_1 = C_1 x(t) + D_1 u(t) \tag{6}$$

For switching mode (b),

$$\dot{x}(t) = A_2 x(t) + B_2 u(t) \tag{7}$$

$$y_2 = C_2 x(t) + D_2 u(t) \tag{8}$$

Where; $x(t) = \begin{bmatrix} i_L(t) \\ v_c(t) \end{bmatrix}$, $u(t) = V_s$, $y(t) = V_{out}(t)$

$$A_1 = \begin{bmatrix} -\frac{1}{L}\left(r_{son} + r_L + \frac{r_c.R_L}{R_L+r_c}\right) & -\frac{R_L}{L(R_L+r_c)} \\ \frac{R_L}{C(R_L+r_c)} & -\frac{1}{C(R_L+r_c)} \end{bmatrix}, B_1 = \begin{bmatrix} \frac{1}{L} \\ 0 \end{bmatrix}, C_1 = \begin{bmatrix} \frac{r_c.R_L}{R_L+r_c} & \frac{R_L}{R_L+r_c} \end{bmatrix}, \text{and } D_1 = 0$$

$$A_2 = \begin{bmatrix} -\frac{1}{L}\left(r_{son} + r_L + \frac{r_c.R_L}{R_L+r_c}\right) & -\frac{R_L}{L(R_L+r_c)} \\ \frac{R_L}{C(R_L+r_c)} & -\frac{1}{C(R_L+r_c)} \end{bmatrix}, B_2 = \begin{bmatrix} 0 \\ 0 \end{bmatrix}, C_2 = \begin{bmatrix} \frac{r_c.R_L}{R_L+r_c} & \frac{R_L}{R_L+r_c} \end{bmatrix}, \text{and } D_2 = 0$$

To derive an average model of the power converter over one switching cycle, the equations corresponding to ON state and OFF state are time weighted and averaged as given in Eqs. (9 and 10).

$$\dot{x}(t) = Ax(t) + Bu(t) \tag{9}$$

$$y(t) = Cx(t) + Du(t) \tag{10}$$

Here A, B, C, and D are given by:

$$A = A_1 d(t) + A_2(1 - d(t)) \tag{11}$$

$$B = B_1 d(t) + B_2(1 - d(t)) \tag{12}$$

$$C = C_1 d(t) + C_2(1 - d(t)) \tag{13}$$

$$D = D_1 d(t) + D_2(1 - d(t)) \tag{14}$$

Where; d: is the duty ratio.

Now, consider there is a small signal variation $\hat{d}$ to the duty ratio d that will cause a small variation $\hat{x}$ of the state variable x and a small variation $\hat{u}$ of input voltage u. Therefore, the small signals variations are symbolized as follows:

$$x(t) = x(t) + \hat{x}(t) \tag{15}$$

$$d(t) = d(t) + \hat{d}(t) \tag{16}$$

$$u(t) = u(t) + \hat{u}(t) \tag{17}$$

Where $\hat{x}$ is a small-signal variation in the DC or steady-state component x, $\hat{d}$ is a small signal variation in the steady-state or DC component duty-ratio d and $\hat{u}$ is a small-signal variation in the DC input voltage u. Therefore, Eq. (9) becomes:

$$(x(t) + \dot{\hat{x}}(t)) = \left[\left(d(t) + \hat{d}(t)\right)A_1 + (1 - d(t) - \hat{d}(t))A_2\right][x(t) + \hat{x}(t)] + \left[\left(d(t) + \hat{d}(t)\right)B_1 + (1 - d(t) - \hat{d}(t))B_2\right][u(t) + \hat{u}(t)] \tag{18}$$

To simplify Eq. (18) the steady state part equals to zero ($\dot{x} = 0$) and also ignoring the nonlinear term. Therefore, Eq. (18) can be rewritten as in Eq. (19).

$$\dot{\hat{x}}(t) = A\hat{x}(t) + B\hat{u}(t) + [(A_1 - A_2)x(t) + (B_1 - B_2)u(t)]\hat{d}(t) \tag{19}$$

Similarly, Eq. (10) becomes:

$$\hat{y}(t) = C\hat{x}(t) + D\hat{u}(t) + [(C_1 - C_2)x(t) + (D_1 - D_2)u(t)]\hat{d}(t) \tag{20}$$

Equation (21) can be obtained by solving Eqs. (19 and 20) and using Laplace transform with some rearrangements, the transfer function of the buck converter model can be obtained as follows:

$$\frac{V_{out}(s)}{\hat{d}(s)} = C(SI - A)^{-1}[(A_1 - A_2)X(s) + (B_1 - B_2)U(s)] \tag{21}$$

3. ADAPTIVE PID CONTROLLER DESIGN

A PID controller is commonly employed in several industrial applications because it is easy to implement, eliminates the steady state error of the step input response due to the integral action effect, and its parameters can be adjusted easily and separately. The proposed block diagram of this adaptive controller which consists of a PID controller and bat algorithm is shown in **Fig. 2**.
The PID controller equation in the time domain can be described by Eq. (22) **(Saud and Mohammed, 2017** and **Abbas and Sami, 2018):**

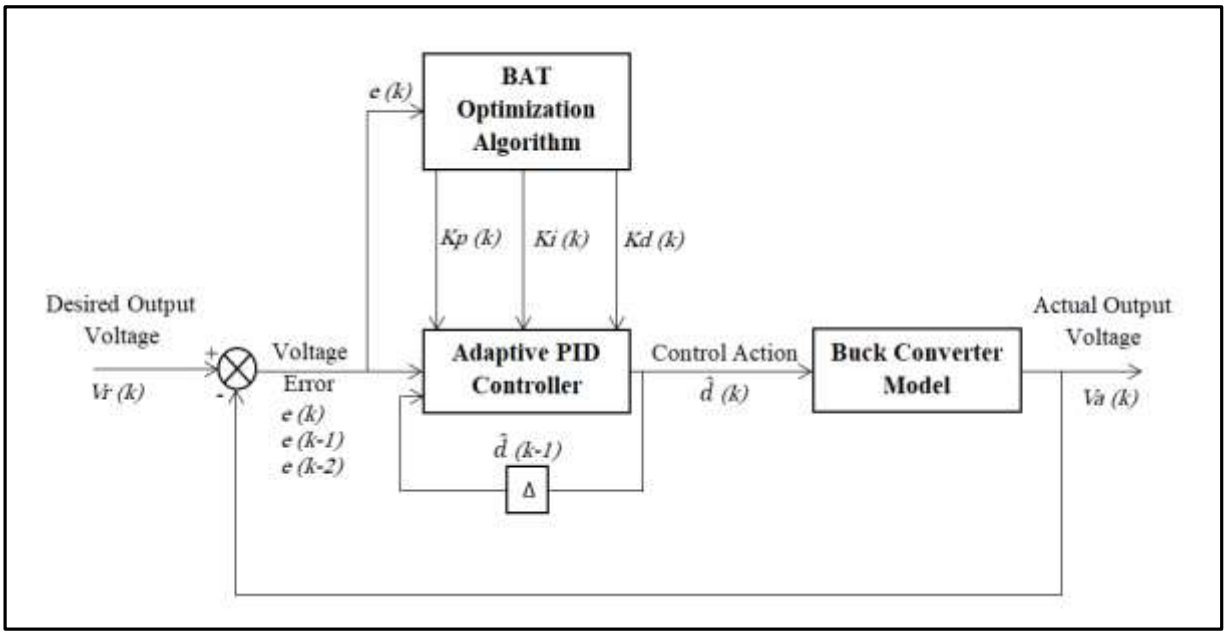

Figure 2. The proposed block diagram of the adaptive PID controller for buck converter system.

$$\hat{d}(t) = kp\, e(t) + ki \int_0^t e(t)\, dt + kd\, \frac{de(t)}{dt} \tag{22}$$

Where, kp is the proportional parameter, ki is the integration parameter, kd is the differentiation parameter, $e(t)$ is the error signal and $\hat{d}(t)$ is the control action.
The discrete-time equation of the PID controller can be obtained by taking the first derivative of Eq. (22) as follows:

$$\dot{\hat{d}}(t) = kp\, \dot{e}(t) + ki\, e(t) + kd\, \ddot{e}(t) \tag{23}$$

Applying the Backward difference formula to $\dot{u}(t)$, $\dot{e}(t)$ and $\ddot{e}(t)$ as follows:

$$\dot{\hat{d}}(t) = \frac{\hat{d}(k) - \hat{d}(k-1)}{ts} \tag{24}$$

$$\dot{e}(t) = \frac{e(k) - e(k-1)}{ts} \tag{25}$$

$$\ddot{e}(t) = \frac{\dot{e}(k) - \dot{e}(k-1)}{ts} \tag{26}$$

Where; ts is the sampling time.

Substitute Eqs. (24, 25, and 26) in Eq. (23) gives Eq. (27) as follows:

$$\frac{\hat{d}(k) - \hat{d}(k-1)}{ts} = kp\, \frac{e(k) - e(k-1)}{ts} + ki\, e(k) + kd\, \frac{\dot{e}(k) - \dot{e}(k-1)}{ts} \tag{27}$$

Applying the Backward difference formula on $\dot{e}(k)$ and $\dot{e}(k-1)$ in Eq. (27) gives Eq. (28) as follows:

$$\frac{\hat{d}(k)-\hat{d}(k-1)}{ts} = kp\ \frac{e(k)-e(k-1)}{ts} + ki\ e(k) + kd\ \frac{\frac{e(k)-e(k-1)}{ts} - \frac{e(k-1)-e(k-2)}{ts}}{ts} \quad (28)$$

Solving for $u(k)$ finally gives the discrete-time PID controller as in Eq. (29):

$$\hat{d}(k) = \hat{d}(k-1) + Kp\left(e(k) - e(k-1)\right) + Ki\ e(k) + Kd\ (e(k) - 2e(k-1) + e(k-2)) \quad (29)$$

where; $Kp = kp$, $Ki = ki * ts$, and $Kd = \frac{kd}{ts}$

The PID controller structure based on Eq. (29) for controlling the output voltage of a buck converter system is shown in **Fig. 3.**

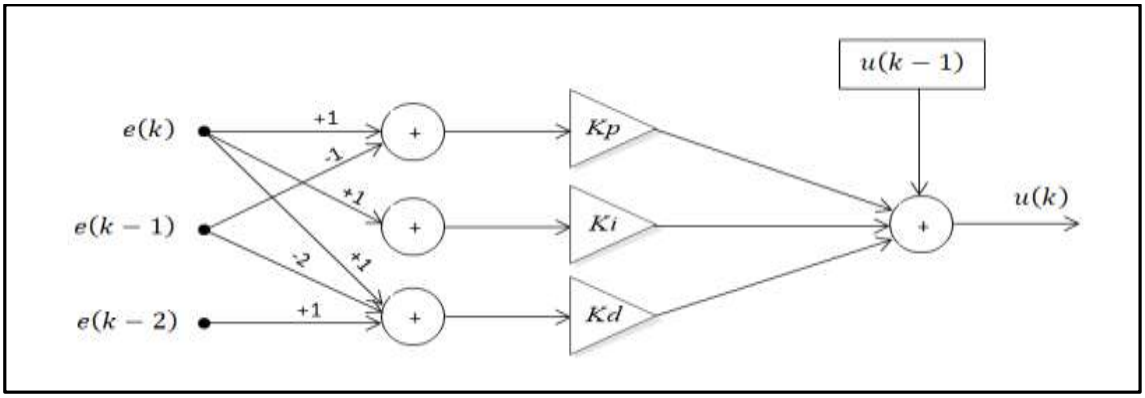

Figure 3. The structure of the PID controller.

4. BAT OPTIMIZATION ALGORITHM

Bat algorithm is a relatively new meta-heuristic swarm algorithm for global optimization and it is introduced and developed in 2010 by Xin-She Yang. This algorithm is inspired by the echolocation behavior of the microbats, with varying pulse rates of emission and loudness **(Yang, 2013)**.

The bat optimization algorithm can be explained in three main rules: The first rule is estimating the optimal distance to the food using the echolocation phenomena. In the Second rule, the bats fly randomly in the search space with a certain velocity at a certain position with a fixed frequency. However, the wavelength and bat loudness can vary according to their distance between food and the entire bat current position. Finally, the third rule followed by bat algorithm is linearly decreasing the behavior of bat loudness factor (**Nor'Azlan, et al., 2018)**.

The steps of bat optimization algorithm are given as follows **(Nor'Azlan, et al., 2018** and **Sambariya and Paliwal, 2016)**:

Step 1: Initialize the algorithm parameters such as dimension of the problem (dim), population size (N), maximum number of maximum iterations ($Iter$), minimum frequency (f_{min}), maximum frequency (f_{max}), loudness of bats (A_l), the initial Pulse emission rate (ro), pulse emission rate of bats (Υ), and the initial velocity of bats (v).

Step 2: In bat algorithm, each bat position represents a feasible solution and the initial population for each bat can be generated randomly as in Eq. (30):

$$x_{ij} = x_j^l + rand() * (x_j^u - x_j^l) \quad (30)$$

Where; $i = 1, \dots, N$, $j = 1, \dots, dim$, and x_j^l and x_j^u are the lower and upper boundaries of dimension j respectively.

Step 3: Evaluate the cost function (MSE) as in Eq. (31) for each bat and store the results in $(cost)$ vector.

$$MSE(i) = \frac{1}{N}\sum_{i=1}^{N}(R - Y)^2 \quad (31)$$

Where; R is the desired signal, and Y is the output signal.

Step 4: Find the best bat position x^* which is the bat that has the smallest (MSE) value among all bats in $(cost)$ vector and consider its (MSE) value as (f_{min}).

Step 5: Update the frequency, velocity, and position for the i^{th} bat as shown in Eqs. (32, 33, and 34) respectively.

$$f_{i=}f_{min} + (f_{max} - f_{min}) * rand() \quad (32)$$

$$v_i^{ii} = v_i^{ii-1} + \left(x_i^{ii-1} - x^*\right) * f_i \quad (33)$$

$$x_i^{ii} = x_i^{ii-1} + v_i^{ii} \quad (34)$$

Where; $ii = 1, \dots, Iter$.

Step 6: A local search is carried out if the rate of pulse emission by the i^{th} bat (Y_i) is less than a randomly generated number, a new solution is generated for the i^{th} bat via a random walk to improve the variability of the possible solutions as in Eq. (35).

$$x_i^{new} = x^* + \epsilon * < A_l >^{ii} \quad (35)$$

Where; ϵ is a scaling factor generated randomly of interval [-1, 1], and $< A_l >^{ii}$ is the average loudness of all bats at ii iteration.

Step 7: Evaluate the cost function value (MSE_i) for the i^{th} bat as in Eq. (31) and store the result in $(costn)$ variable.

Step 8: For the i^{th} bat, if its new cost function value $(costn_i)$ is smaller than its previous cost function value and its loudness (A_{l_i}) is bigger than a randomly generated number then the new values of its cost function, loudness and Pulse rate are calculated as in Eqs. (36, 37, and 38) respectively.

$$cost_i = costn \tag{36}$$

$$A_{l_i} = \alpha * A_{l_i} \tag{37}$$

$$Y_i = ro * (1 - exp(-\beta * ii)) \tag{38}$$

Where; α and β are constants between [0, 1].

Step 9: For the i^{th} bat, if its $(costn_i)$ is smaller than f_{min} then the best bat position (x^*) and minimum frequency (f_{min}) can be updated according to the Eqs. (39 and 40).

$$x^* = x_{ij} \tag{39}$$

$$f_{min} = costn_i \tag{40}$$

Step 10: If the maximum number of bats (N) is reached go to Step 11. Otherwise, go to Step 5.

Step 11: Stop if the maximum number of iterations $(Iter)$ is reached. Otherwise, Step 5 to Step 11 is repeated.
The typical bat algorithm flow chart for the adaptive PID controller is shown in **Fig. 4**.

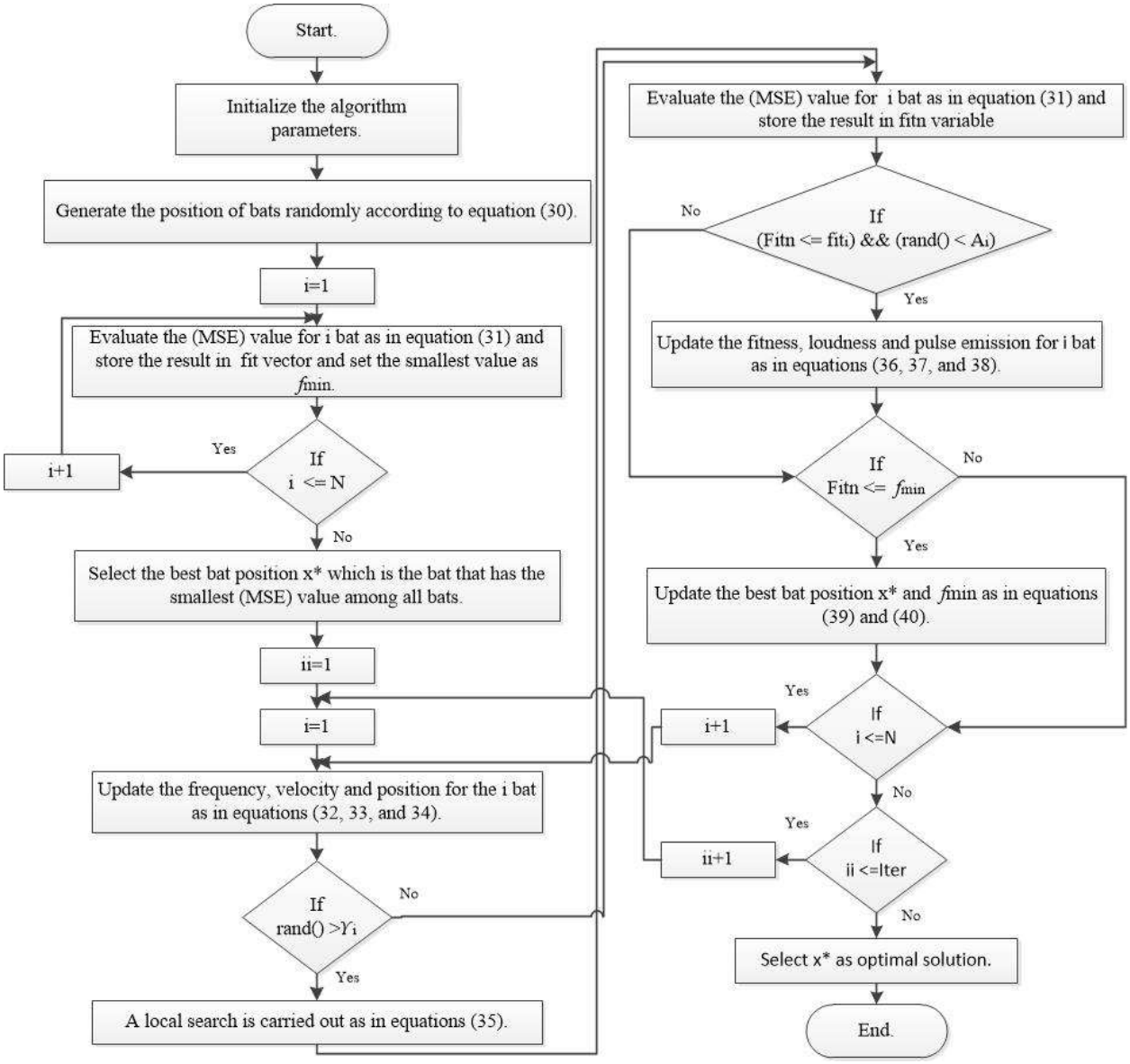

Figure 4. The proposed flow chart of the adaptive PID controller based bat optimization algorithm.

5. SIMULATION RESULTS AND DISCUSSION

The specifications of the Buck converter model are taken from (**Al-Araji, 2017)**as shown in **Table 1**, **(Al-Araji, 2017)**. The on-line bat optimization control algorithm for the PID controller is carried out by using the MATLAB simulation package to obtain the reference output voltage for buck circuit as shown in **Fig. 2**. The time constant of the system is equal to $\tau = 26.14\ \mu sec$ depending on the natural frequency $wn = 3.4699 \times 10^4\ rad/sec$ and the damping ratio $\zeta = 1.1025$ of the Buck converter system. By applying the Shannon theorem, the sampling time of the Buck converter system is equal to $3.6001\ \mu sec$.

Table 1. The buck converter model parameters' values.

Component	Symbol	Value	Unit
The Inductance of The Converter	L	33	μH
The Capacitor of The Converter	C	47	μF
The Load Resistance of The Converter	R_{Load}	2.345	Ω
The Inductor Effective Series Resistance	r_L	66	$m\Omega$
The Capacitor Effective Series Resistance	r_C	70	$m\Omega$
The ON-n-Channel Resistance of MOS Transistors	r_{son}	2.1	Ω
Input Voltage	V_{Supply}	3.75	V
Duty Ratio	d	0.48	-
Switching frequency	f	80	kHz

According to Eq. (21) and the parameters' values of the buck converter model, the transfer function of the buck converter model is described as in Eq. (41).

$$\frac{V_{out}(s)}{\hat{d}(s)} = \frac{7724\ S+2.348\times10^{9}}{S^{2}+7.651\times10^{4}\ S+1.204\times10^{9}} \tag{41}$$

The open-loop step response of the buck converter system output voltage is shown in **Fig. 5**. From this plot; the buck system has a stable response.

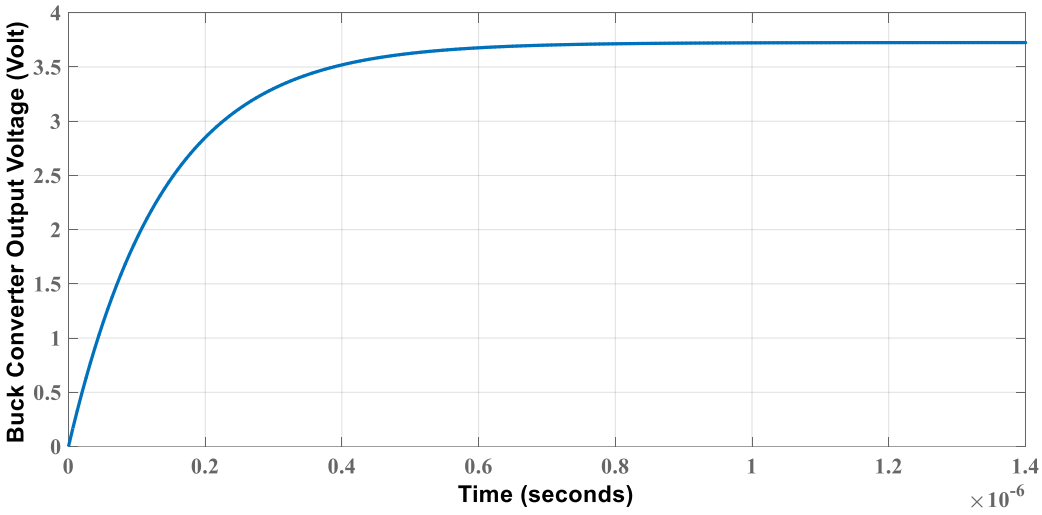

Figure 5. The open loop response of the buck converter model.

In this work, to investigate the performance of the adaptive PID controller shown in **Fig. 2** the on-line bat optimization algorithm methodology has been used. The bat algorithm has the ability to minimize the voltage tracking error with the minimum fitness evaluation number by generating an optimal voltage control action to the buck converter circuit. The bat algorithm parameters used in this control methodology are defined in **Table 2**.

Table 2. The parameters of the bat algorithm.

Parameter	Symbol	Value
The population size	N	30
The maximum number of iterations	$Iter$	100
The dimension of the problem	dim	3
Alpha	α	0.5
Beta	β	0.5
The initial Pulse emission rate	ro	0.001
The minimum frequency	f_{min}	0
The maximum frequency	f_{max}	0.01
The loudness for each bat	A_l	$rand()$
The pulse emission rate for each bat	Υ	$rand()$

The simulation results of the closed loop voltage control system with the variable voltage step change as (2.25, 1.75 and 1.3) volt in the buck converter's desired output voltage based on on-line bat tuning of the PID controller with the zero initial output voltage of the system are depicted in **Figs. 6 to 10**.

The response of the converter output voltage in the proposed controller, (**Al-Araji, 2017** and **Dagher, K., 2018)** in each voltage step change has a very small rising time, settling time, and overshoot in the transient state while the value of the error is equal to zero at the steady-state, as depicted in **Fig. 6** and **Table 3**.

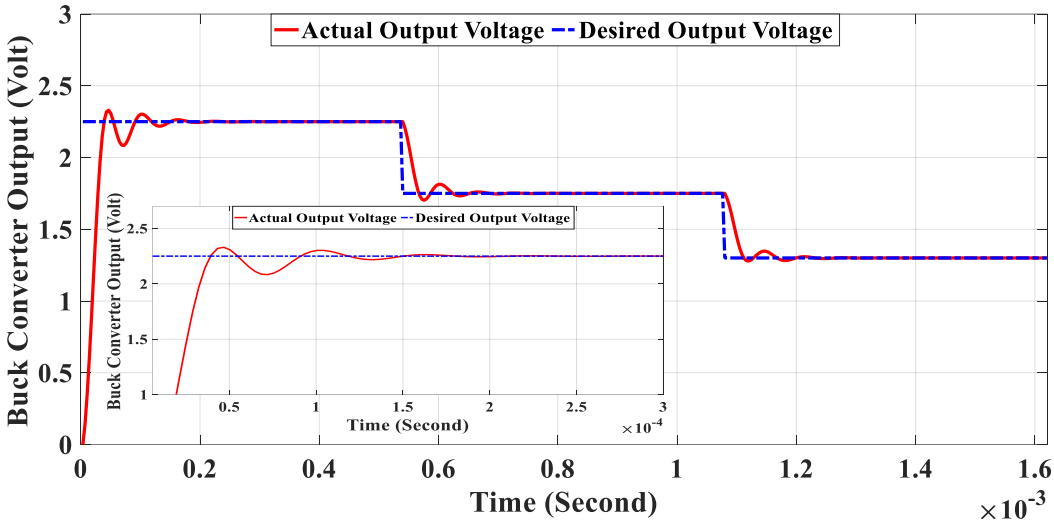

Figure 6. The Output voltage for buck converter system.

Table 3. The dynamic behavior of the buck converter output voltage with different controllers.

Controller Type	Rising Time (*Tr*)	Settling Time (*Ts*)	Maximum Overshoot (O.S)	Steady state Error (*Es.s*)
The proposed Controller	0.393×10^{-4} sec	2×10^{-4} sec	7 %	0
Al-Araji, 2017	1.25×10^{-4} sec	2.5×10^{-4} sec	3 %	0
Dagher, K., 2018	1.26×10^{-4} sec	2.88×10^{-4} sec	5 %	0

In **Fig. 7**, the voltage error signal of the closed loop buck converter controller system was a small value in the transient and it has become zero at the steady state.

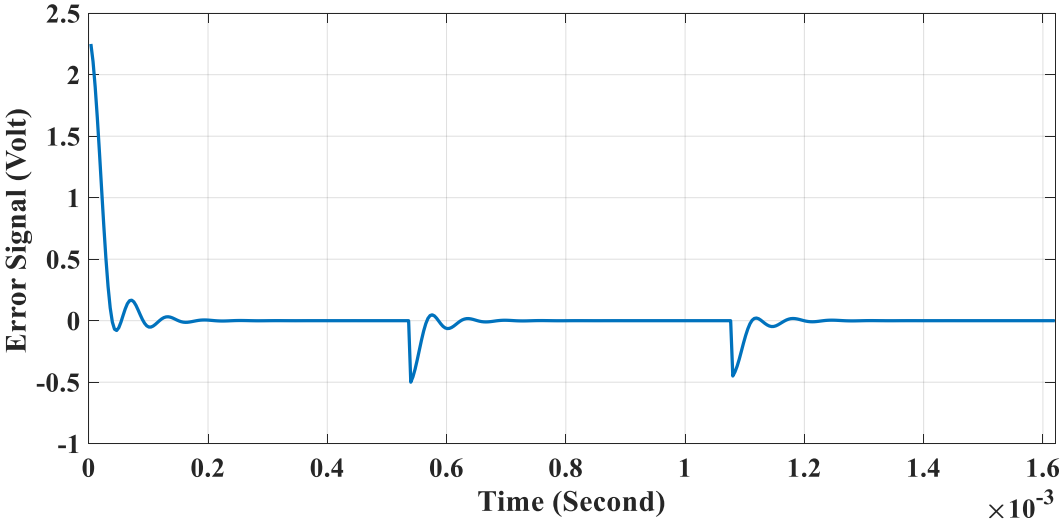

Figure 7. The Voltage error signal.

The control action response In **Fig. 8** of the adaptive PID controller was smooth without oscillation response, no spikes behavior and the action response did not exceed to the saturation state of the input voltage (3.75) volt.

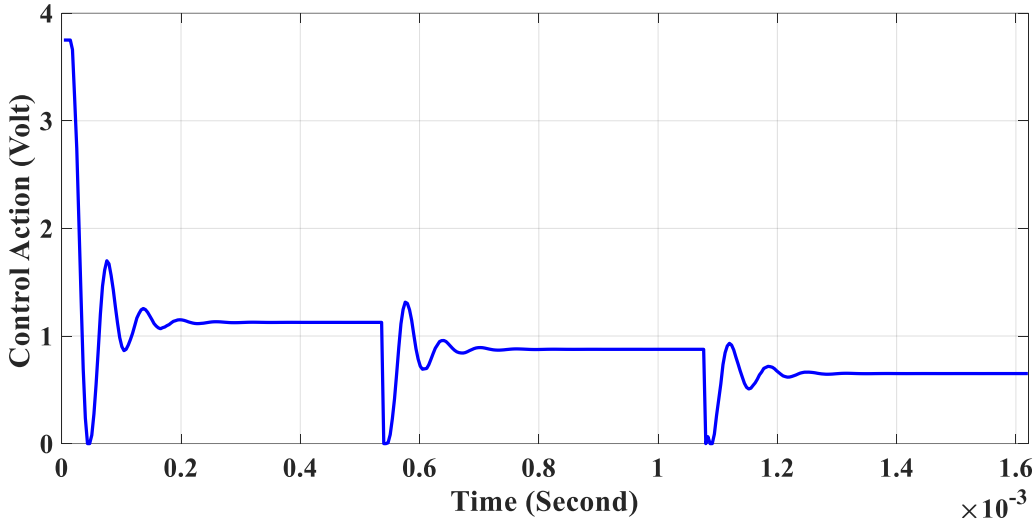

Figure 8. The voltage control action.

Fig.9 clearly shows the improved Mean Square Error (MSE) performance index of the buck model based on the on-line bat tuning control methodology at 450 samples.

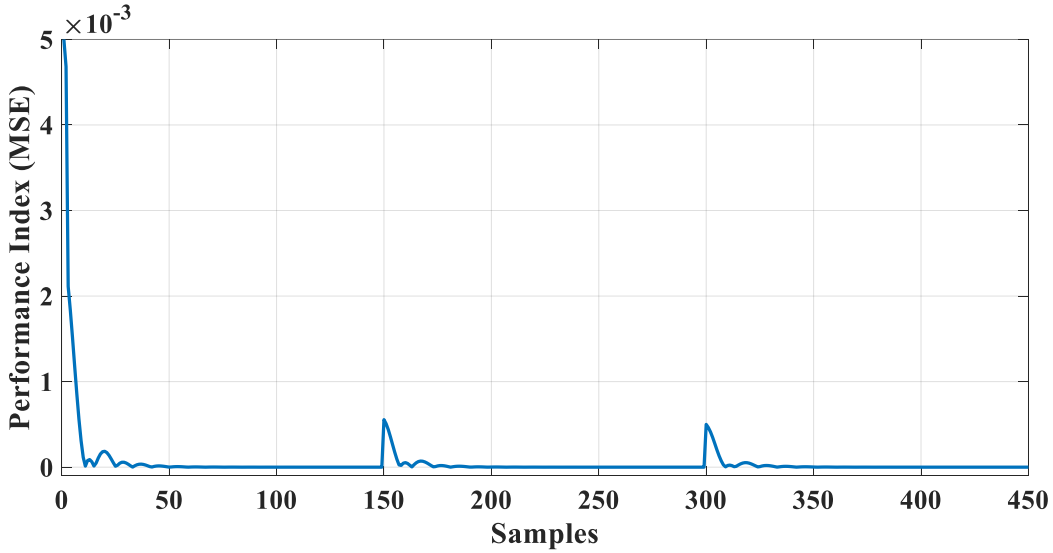

Figure 9. The On-line performance index (MSE).

The on-line tuning gains of the proposed adaptive controller Kp, Ki, and Kd) at each sample by using bat optimization algorithm are depicted in **Figs. 10 a, b, and c**, respectively.

(a)

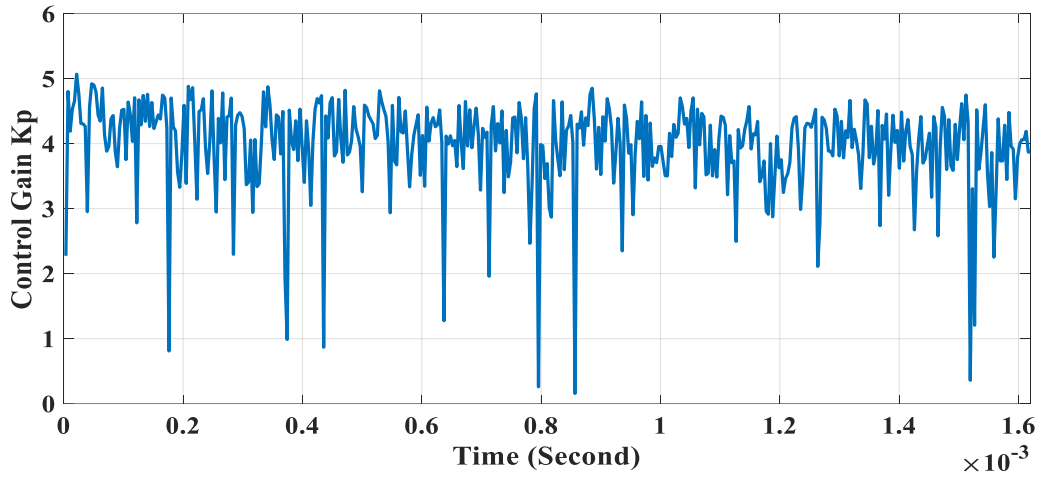

(b)

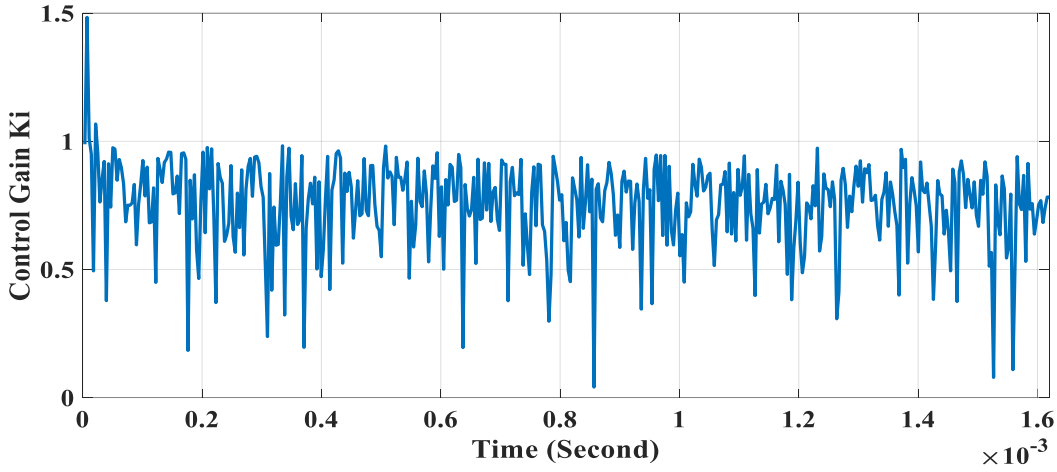

(c)

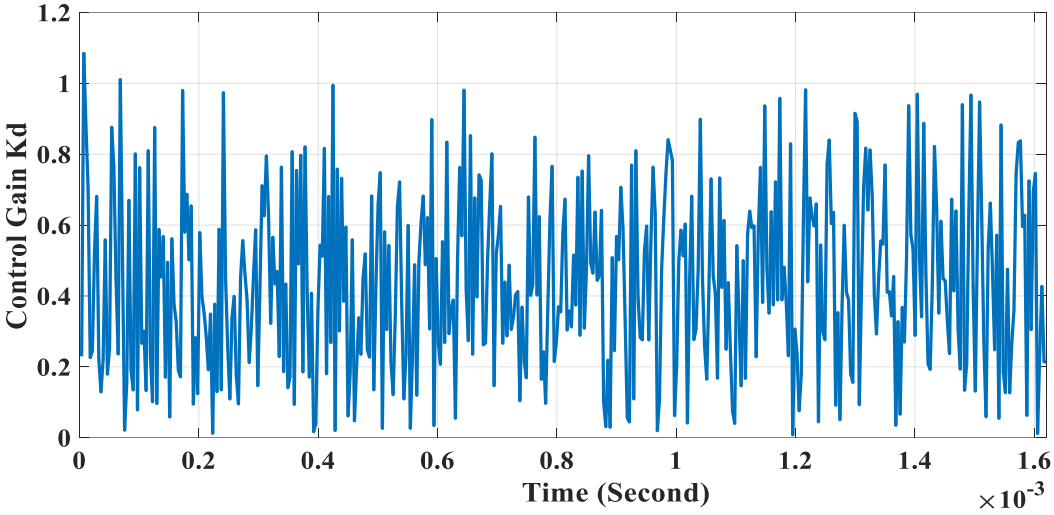

Figure 10. The on-line tuning control parameters: (a) Kp (b) Ki and (c) Kd.

To investigate that the closed loop buck converter system has a robust performance for boundary disturbance a variable load resistance is added by decreasing 57% and 14.7% from its value at ($0.288\ msec$) and ($0.864\ msec$), respectively. According to Eq. (21) and the parameters' values of the buck converter model, the transfer function of the buck converter model after decreasing the load resistance by 57% is described as in Eq. (42).

$$\frac{V_{out}(s)}{\hat{d}(s)} = \frac{7434\ S+2.26\times10^{9}}{S^{2}+8.75\times10^{4}\ S+1.908\times10^{9}} \tag{42}$$

The time constant of the system is equal to $\tau = 22.857\ \mu sec$ depending on the natural frequency $wn = 4.3681 \times 10^{4}$ *rad/sec* and the damping ratio $\zeta = 1.0016$ of the Buck converter system. By applying the Shannon theorem, the sampling time of the Buck converter system is equal to $3.1479\ \mu sec$.

Similarly, according to Eq. (21) and the parameters' values of the buck converter model, the transfer function of the buck converter model after decreasing the load resistance by 14.7 % is described as in Eq. (43).

$$\frac{V_{out}(s)}{\hat{d}(s)} = \frac{7686\ S+2.336\times10^{9}}{S^{2}+7.796\times10^{4}\ S+1.298\times10^{9}} \tag{43}$$

The time constant of the system is equal to $\tau = 25.654\ \mu sec$ depending on the natural frequency $wn = 3.6028 \times 10^{4}$ *rad/sec* and the damping ratio $\zeta = 1.0819$ of the Buck converter system. By applying the Shannon theorem, the sampling time of the Buck converter system is equal to $3.5331\ \mu sec$.

The output voltage response of the buck converter system to voltage step change (2.25 and 1.75) volt has small over shoot at ($0.335\ msec$) and ($0.9144\ msec$), respectively with very small oscillation during adding disturbance but at the steady state, the error is equal to zero value as shown in **Fig. 11 a.** The small value of the error voltage signal between the reference voltage and the output voltage of the buck converter system is shown in **Fig. 11 b**, the error has a small value at the transient state and in the steady state, the error becomes very close to zero with a very small oscillation. **Fig. 11 c** shows the response of the control action which has a capability to track the error voltage signal of the buck converter system to follow the reference voltage as step change and reduce the effect of the load resistance disturbance.

(a)

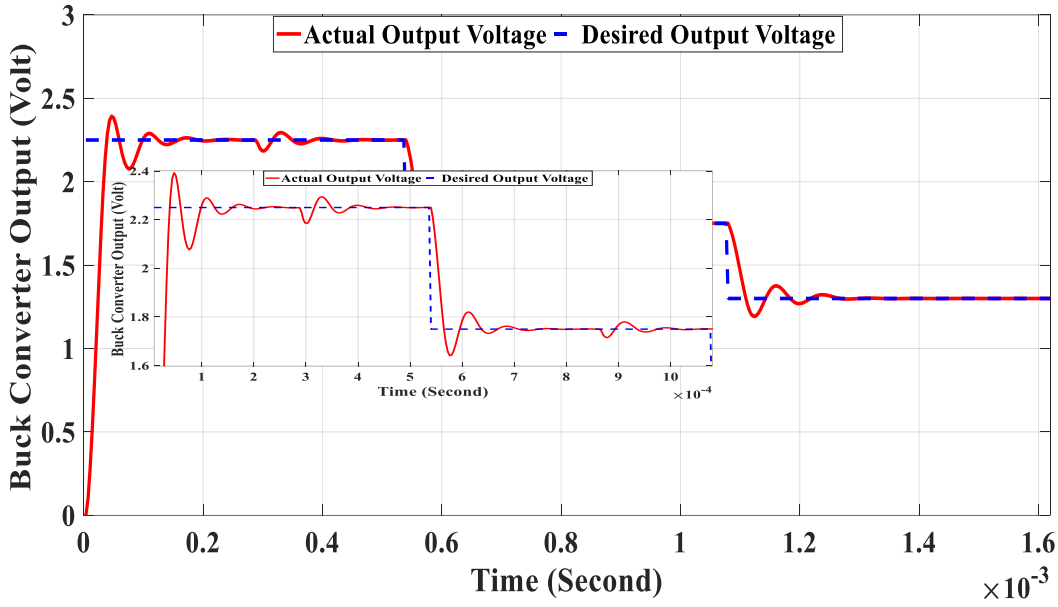
Actual Output Voltage
Desired Output Voltage
Buck Converter Output (Volt)
Time (Second)
×10-3
Actual Output Voltage
Desired Output Voltage
Buck Converter Output (Volt)
Time (Second)
×10-4

(b)

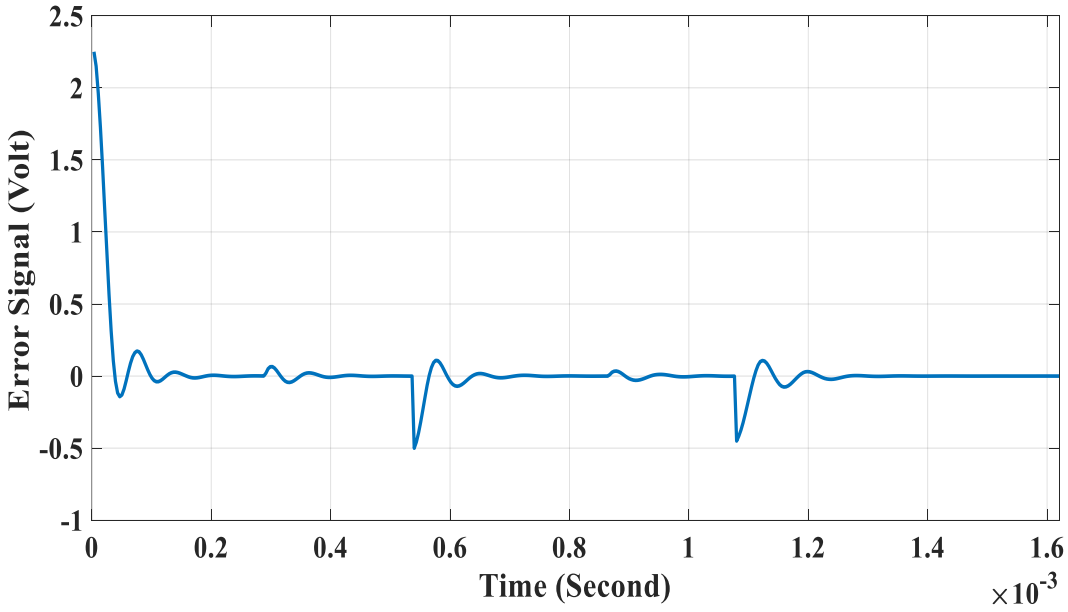
Error Signal (Volt)
Time (Second)
×10-3

(c)

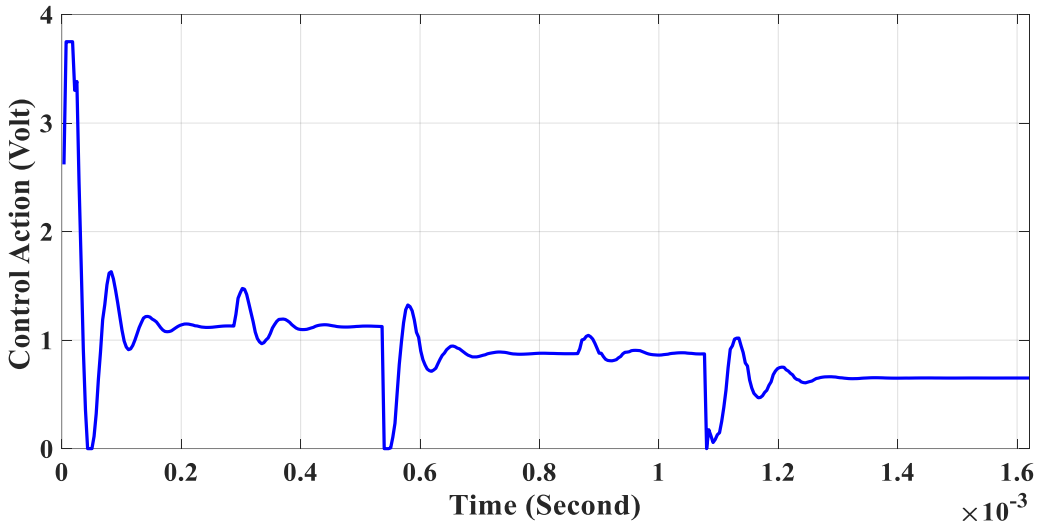

Figure 11. Simulation results of the proposed controller with disturbance effect: (a) The output voltage for buck converter system (b) The Voltage error signal (c) The voltage control action.

Fig. 12 clearly shows the improved MSE performance index of the buck model based on the on-line bat tuning control methodology at 450 samples during adding disturbance.

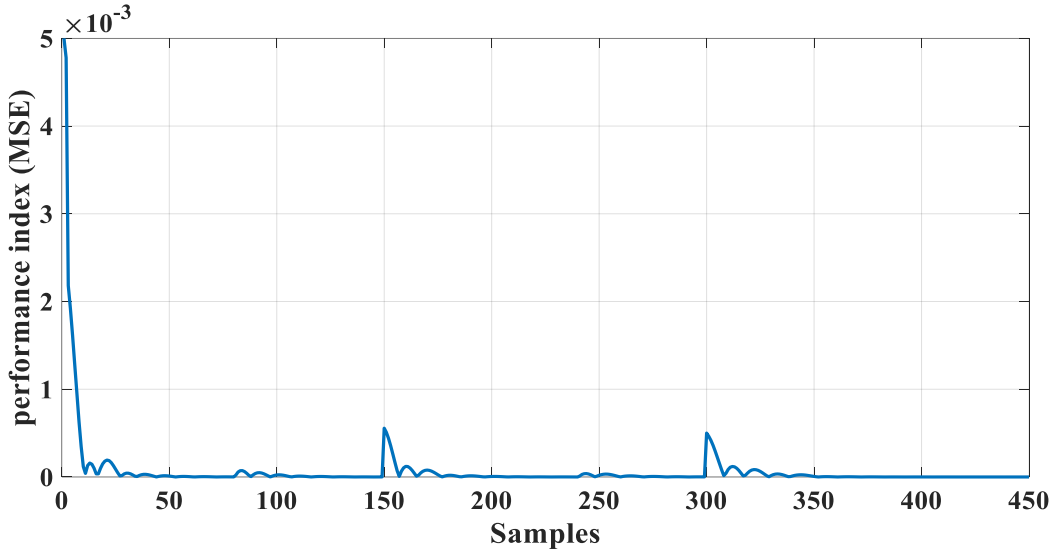

Figure 12. The On-line performance index (MSE) during adding disturbance.

Finally, the on-line tuning parameters of the proposed controller (Kp, Ki, and Kd) during adding disturbance at each sample by using bat optimization algorithm are depicted in **Figs. 13 a, b, and c**, respectively.

(a)

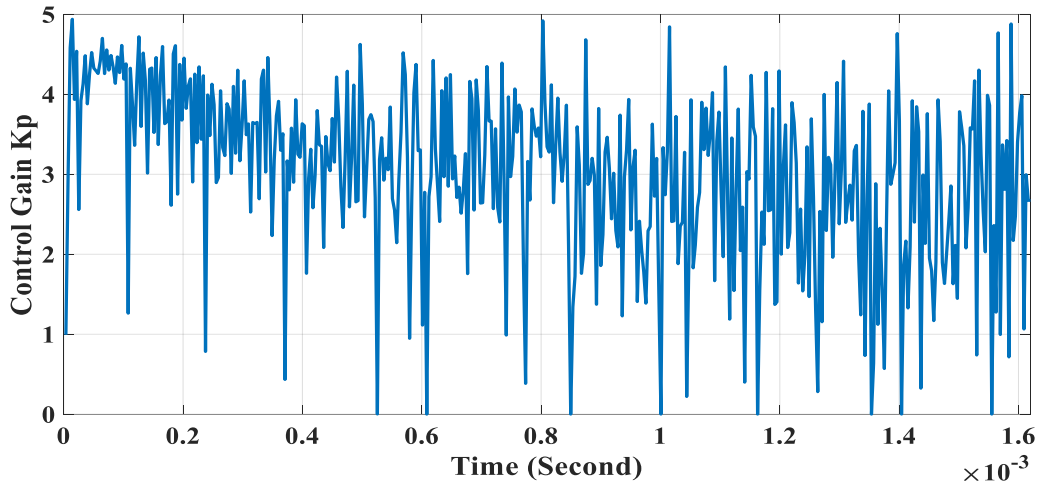

(b)

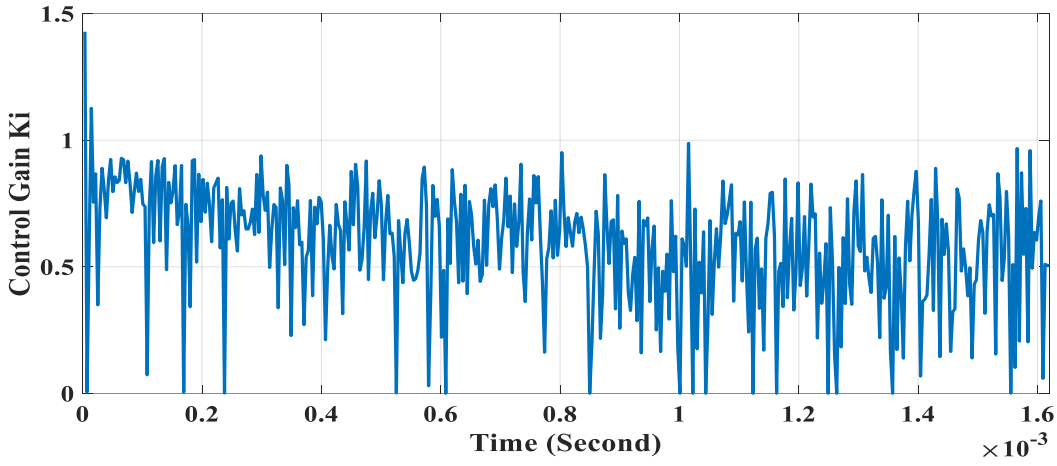

(c)

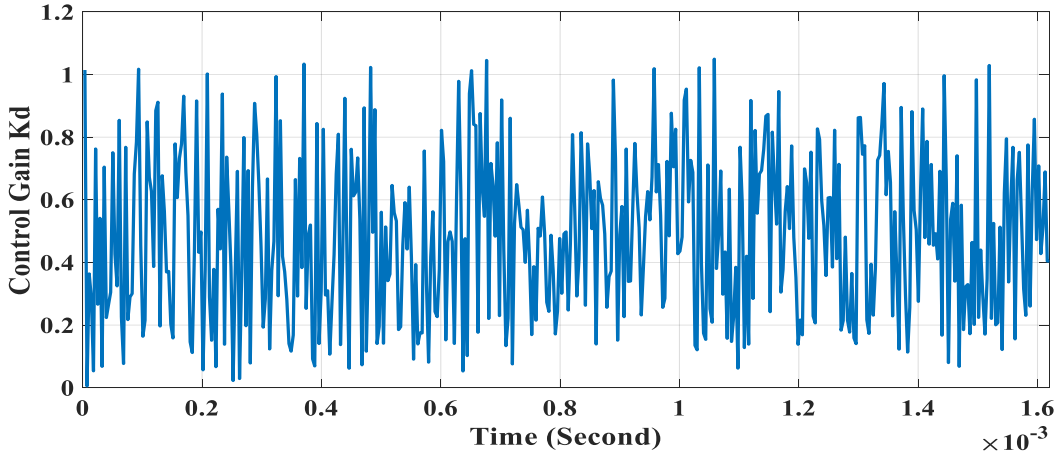

Figure 13. The on-line tuning control parameters during adding disturbance: (a) Kp (b) Ki (c) Kd.

6. CONCLUSIONS

The numerical Matlab simulation results based on the on-line tuning bat optimization algorithm of the PID controller have been demonstrated in this work for the synchronous buck converter model. The proposed control system has the following capabilities:

- The on-line bat tuning optimization algorithm has the ability of quickly pick up of the optimal gains of the controller with the minimum fitness evaluation number.
- A proper voltage control action was obtained without a saturation voltage state for the input voltage of the buck converter system which equals (3.75) volt.
- An excellent tracking of the desired output voltage with the minimum voltage tracking error was achieved.
- Strong adaptability performance was achieved by changing the desired output voltage level.
- High robustness performance was obtained by changing the load resistance value as a disturbance effect to the buck converter model.
- A desirable time response specifications was achieved by minimizing the rising time to (0.393×10^{-4} sec) and the settling time to (2×10^{-4} sec) in the transient response and minimizing the voltage tracking error of the system output to ($zero$) volt at the steady state response when compared with the other controllers results.

REFERNCES

- Abbas, N. and Sami, A., 2018. Tuning of PID Controllers for Quadcopter System using Cultural Exchange Imperialist Competitive Algorithm. *University of Baghdad, Journal of Engineering, 24 (2),* pp., 80- 99.
- Abed, W., Imran, O., and Jbarah, A., 2018. Voltage Control of Buck Converter- Based Ant Colony Optimization for Self Regulating Power Supplies. *Medwell Journals, Journal of Engineering and Applied Sciences, 13 (12),* pp., 4463-4467.
- Al-Araji, A., 2017. Development of an On-Line Self-Tuning FPGA-PID-PWM Control Algorithm Design for DC-DC Buck Converter in Mobile Applications. *University of Baghdad, Journal of Engineering, 23 (8),* pp., 84- 106.
- Chafekar, N., and Mate, U., 2018. Design and Simulations of Sliding Mode Controller for DC–DC Buck Converter. *International Journal for Innovative Research in Science & Technology (IJIRST), 4 (12),* pp., 38-45.
- Chander, S., Agarwal, P., and Gupta, I., 2013. ASIC and FPGA based DPWM Architectures for Single-Phase and Single-Output DC-DC Converter: a Review. *Central European Journal of Engineering, 19 (4),* pp., 620-643.
- Dagher, K., 2018. Modified Elman Neural-PID Controller Design for DC-DC Buck Converter System Based on Dolphin Echolocation Optimization. *Al-Khwarizmi Journal of Engineering, 14 (3),* pp., 129-140.
- Danayiyen, Y., Altas, I., and SAHİN, E., 2017. Model Predictive Control of a DC-DC Buck Converter. *Sigma J Eng & Nat Sci 8 (2),* pp., 91-97.
- Garg, M., Hote, Y. and Pathak, M., 2015. Design and Performance Analysis of a PWM DC-DC Buck Converter Using PI-Lead Compensator. *Arabian Journal for Science and Engineering, 40 (12),* pp., 3607-3626.

- Kalita, P., Saikia, M., and Singh, N., 2015. Adaptive Control Techniques for DC-DC Buck Converter. *International Journal of Engineering Sciences & Research Technology, 4 (6),* pp., 185-193.
- Kim, K-H, Kong, B-S and Jun, Y-H, 2012. Adaptive Frequency-Controlled Ultra-Fast Hysteretic Buck Converter for Portable Devices. *International Conference of IEEE on SoC Design,* pp., 5-8.
- Lakshmi, S., and Raja, T., 2014. Design and implementation of an observer controller for a buck converter. *Turkish Journal of Electrical Engineering & Computer Sciences, 22 (3),* pp., 562-572.
- Lv, L., Chang, C., Zhou, Z., and Yuan, Y., 2013. An FPGA-Based Modified Adaptive PID Controller for DC/DC Buck Converters. *Journal of Power Electronics, 15 (2),* pp., 346-355.
- Mazlan, M., Haqkimi, N., Charin, C., Fairuz, N., Izni, N.,and Annuar, M., 2015. State Feedback Controller Using Pole Placement Method for Linear Buck Converter to Improve Overshoot and Settling Time. *Applied Mechanics and Materials 793 (1),* pp. 211-215.
- Mohan, N., Undeland, T., and Robbins, W., 1995. *Power Electronics: Converters, Applications, and Design*. John Wiley & Sons, In., 2nd edition, New York.
- Nizami, T., and Mahanta, C., 2014. Adaptive Backstepping Control for DC-DC Buck Converters using Chebyshev Neural Network. *Annual IEEE India Conference (INDICON),* pp., 1-5.
- Nor'Azlan, N., Selamat, N., and Yahya N., 2018. Multivariable PID controller design tuning using bat algorithm for activated sludge process. *IOP Conference Series: Materials Science and Engineering, 342 (1),* pp., 1-9.
- Sambariya, D., and Paliwal, D., 2016. Design of PIDA Controller Using Bat Algorithm for AVR Power System. *Advances in Energy and Power, 4 (1),* pp., 1-6.
- Saud, L. and Mohammed, R., 2017. Performance Evaluation of a PID and a Fuzzy PID Controllers Designed for Controlling a Simulated Quadcopter Rotational Dynamics Model. *University of Baghdad, Journal of Engineering, 23 (7),* pp., 74- 93.
- Tapou, M., Al-Raweshidy, H., Abbod, M. and Al-Kindi, M., 2011. A Buck Converter for DVS Compatible Processors in Mobile Computing Applications Using Fuzzy Logic Implemented in a RISC Based Microcontroller. *The 2nd Internation Conference on Circuit and System Control Signal. Prague, Czech,* pp., 135-139.
- Themozhi, G., and Reddy S., 2014. On Chip Pulse Width Modulator and Dead Time Controller in Bidirctional DC to DC Converter for Aero Space Applications. *Arabian Journal for Science and Engineering, 39 (2),* pp., 957-966.
- Yang, X-S, 2013. Bat Algorithm: Literature Review and Applications. *International Journal of Bio-Inspired Computation, 5 (3),* pp., 141-149.